J. Fluid Mech. (1984), *vol.* 143, *pp.* 1–21
Printed in Great Britain

Stirring by chaotic advection

By HASSAN AREF
Division of Engineering, Brown University, Providence, Rhode Island 02912

(Received 30 March 1983)

In the Lagrangian representation, the problem of advection of a passive marker particle by a prescribed flow defines a dynamical system. For two-dimensional incompressible flow this system is Hamiltonian and has just one degree of freedom. For unsteady flow the system is non-autonomous and one must in general expect to observe chaotic particle motion. These ideas are developed and subsequently corroborated through the study of a very simple model which provides an idealization of a stirred tank. In the model the fluid is assumed incompressible and inviscid and its motion wholly two-dimensional. The agitator is modelled as a point vortex, which, together with its image(s) in the bounding contour, provides a source of unsteady potential flow. The motion of a particle in this model device is computed numerically. It is shown that the deciding factor for integrable or chaotic particle motion is the nature of the motion of the agitator. With the agitator held at a fixed position, integrable marker motion ensues, and the model device does not stir very efficiently. If, on the other hand, the agitator is moved in such a way that the potential flow is unsteady, chaotic marker motion can be produced. This leads to efficient stirring. A certain case of the general model, for which the differential equations can be integrated for a finite time to produce an explicitly given, invertible, area-preserving mapping, is used for the calculations. The paper contains discussion of several issues that put this regime of *chaotic advection* in perspective relative to both the subject of turbulent advection and to recent work on critical points in the advection patterns of steady laminar flows. Extensions of the model, and the notion of chaotic advection, to more realistic flow situations are commented upon.

1. Perspectives in the advection problem

The problem of advection is traditionally addressed using one of two well-established points of view. In the first of these, the Eulerian representation, the advected property is described by a scalar field $\theta(\boldsymbol{x}, t)$ which evolves according to an equation of the form

$$\frac{\partial \theta}{\partial t} + \boldsymbol{u} \cdot \nabla \theta = \kappa \Delta \theta. \tag{1}$$

In this equation the advecting velocity field $\boldsymbol{u}(\boldsymbol{x}, t)$ is a prescribed function of spatial coordinates $\boldsymbol{x} = (x, y, z)$ and time t. The diffusivity κ is frequently taken to be constant. The basic equation (1) is obviously linear in θ, a fact that occasionally but repeatedly spawns the erroneous conclusion that the field configuration of θ is at worst as complicated as that of $\boldsymbol{u}$. Indeed, as we shall see later, even a very simple and regular flow field $\boldsymbol{u}$ may induce advection patterns that are highly complex. Within the framework of (1) we may distinguish laminar and turbulent advection according to the nature of the flow field $\boldsymbol{u}$. Conventionally, theoretical treatments

introduce a completely deterministic flow when studying problems of laminar advection, whereas studies of turbulent advection, starting with the seminal papers by Taylor (1921) and Richardson (1926), only specify the flow field $\boldsymbol{u}$ probabilistically.

The alternative view of advection is obtained by working in the so-called Lagrangian representation. Here trajectories of individual advected particles are sought by expressing the problem in the form

$$\dot{x} = u(x, y, z, t), \quad \dot{y} = v(x, y, z, t), \quad \dot{z} = w(x, y, z, t), \qquad (2a, b, c)$$

where the components u, v and w of the velocity field $\boldsymbol{u}$ are once again prescribed. Equations (2) reduce the advection problem to a finite-dimensional dynamical system. For turbulent advection this system is governed by stochastic equations of motion. For laminar flow the system (2) is deterministic. Steady laminar flow implies, furthermore, that (2) is autonomous. As they stand, (2) pertain to the non-diffusive case ($\kappa = 0$) of (1). However, owing to the intimate relationship that exists between a random walk and diffusion (see e.g. Chandrasekhar 1943), the stochastic version of (2) can be constructed to correspond closely with the diffusive case of (1). In this paper we shall be concerned primarily with (2) when $\boldsymbol{u}$ is deterministic, two-dimensional, incompressible and unsteady.

The idea of studying advection by employing the Lagrangian representation through (2) is by no means new. In fact, it is an idea intimately related to the kinematic foundations of fluid mechanics. A discussion of the relationship between Eulerian and Langrangian representations is usually found in an early chapter of any textbook on fluid dynamics (see e.g. Lamb 1932, chap. I; Prandtl & Tietjens 1934, chap. V; Batchelor 1967, chap. 2). The main classical result, stated here in 'modern' terms, is that, if the flow is steady, incompressible and two-dimensional, the advection problem (2) is integrable. The well-known argument is, first, that incompressibility implies existence of a stream function $\psi(x, y)$, and, secondly, that pathlines coincide with streamlines for steady flow. The 'modern' statement might include the observation that (2) in this case become

$$\dot{x} = -\frac{\partial \psi}{\partial y}, \quad \dot{y} = \frac{\partial \psi}{\partial x}, \qquad (3)$$

which are just Hamilton's canonical equations for one degree of freedom and hence integrable when autonomous (cf. Whittaker 1937). The terminology of dynamical-systems theory might sway one to call the streamlines 'tori'. This correspondence between the phase-space flow of a Hamiltonian dynamical system and the configuration-space motion of an advected particle (in incompressible, plane fluid flow) consists of more than idle formalism. Indeed it suggests at once that it must be possible to produce instances of (2) (or (3)) with very complicated particle motions by choosing the flow field in such a way that the dynamical system becomes non-integrable. (For a discussion of non-integrability or chaos in Hamiltonian systems see Hénon & Heiles (1964), Arnold & Avez (1968), Moser (1973), Berry (1978) and Lichtenberg & Lieberman (1983).) For two-dimensional incompressible flow it will suffice to let u and v become time-dependent. In particular, the flow field or the stream function need not themselves become very involved. Thus, the regime of advective motion that we envision is properly a subclass of laminar advection, and not turbulent advection, according to our earlier classification. We have a situation in which an innocuous, fully deterministic velocity field, in the Eulerian view, produces

an essentially stochastic response in the Lagrangian advection characteristics of a passive tracer.† It is proposed to call this situation or regime *chaotic advection.*

In the remainder of the paper the possibility of chaotic advection will be corroborated through the study of a highly idealized model of the stirring of a tank of fluid by an agitator. The ingredients of the model are as follows. The fluid is assumed ideal, i.e. inviscid and incompressible, and its motion is completely two-dimensional. The tank thus degenerates to a curve delineating the boundary. The agitator is modelled as a point vortex. This vortex is bound in the sense that its position as a function of time, the 'stirring protocol', is part of the data specifying the problem. Together with appropriate images in the boundary contour, the vortex agitator maintains an unsteady potential flow within the tank. The objective of our study will be to discover within this simple model format which features control the onset of chaos and hence the efficiency of stirring.

The model arises naturally from recent work on systems of a few point vortices, in particular the so-called restricted four-vortex problem (Aref & Pomphrey 1980; Ziglin 1980; for a review see Aref 1983), in which the advection of a single passive marker particle by three (identical) vortices is studied. The present model distils from these earlier investigations the essence of Lagrangian motion in a prescribed potential flow. As already anticipated, we shall find that for a steady flow the dynamics of the advected particle is integrable; for unsteady flow, on the other hand, non-integrable behaviour may ensue. The corollary of this for stirring is that non-integrability leads to efficient stirring or mixing. Parameters yielding integrable advected particle motion, however, lead to regimes of inefficient stirring. In particular, if the agitating vortex in the model is held at a fixed position, indeed if an arbitrary number of agitating vortices are held at arbitrarily chosen fixed positions, the advecting flow field gives integrable particle motion and inefficient stirring. But a single stirring vortex allowed to move in an appropriate manner can yield chaotic advected particle motion and thus highly efficient stirring.

In §2 a mathematical formulation of the model is presented and some simple analytical properties are derived. Two dimensionless parameters governing the problem are identified. In §3 a particular 'stirring protocol' is investigated for which the motion of the advected particle can be integrated over a finite time, thus reducing the ordinary differential equations of §2 to an explicitly given, invertible, area-preserving, transcendental mapping. The model is studied by numerical experiments in §4. By iterating the mapping for different values of the dimensionless parameters, the regimes of regular and chaotic behaviour are identified. Individual particle trajectories (pathlines) and a series of simultaneous positions of many particles (timelines) arranged to correspond to the stirring of an initial cluster of particles are shown.

A discussion of results appears in §5. In particular, it is imperative to spend some time examining, on one hand, the relationship of this paper to earlier work on stirring, advection and entrainment and, on the other, its relation to past and present results in the theory of two-dimensional mappings. Extensions of the model as well as problems left unresolved by the present investigation are also discussed.

Brief accounts of the work presented here have been given elsewhere (Aref 1982*a*, *b*).

† Related ideas in the context of the 'kinematic-dynamo problem' in hydromagnetics have been explored by U. Frisch (private communication), who quotes the early paper by Hénon (1966). See also §5.4.

2. Mathematical formulation of a model of stirring

We are going to assume that the bounding contour is a circle of radius a. Extensions to non-circular contours are trivially possible and are briefly commented upon in §5.3. Using a notational convenience from the theory of point-vortex motion, we shall consider the plane of flow to be part of the complex plane (cf. Friedrichs 1966). Let the agitating vortex be at $z(t)$, its position as a function of time constituting part of the data specifying the problem. The function $z(t)$ is what we referred to in §1 as the *stirring protocol*. For a circular boundary we have just one image at $a^2/\bar{z}(t)$, where the overbar denotes complex conjugation. If the vortex strength of the agitator is Γ, the strength of the image is $-\Gamma$. The flow field is now completely specified.

Into this flow introduce a particle of negligible mass (and vanishing vorticity) at position $\zeta(t)$. Its equation of motion becomes

$$\dot{\bar{\zeta}} = \frac{\Gamma}{2\pi i}\left\{(\zeta - z)^{-1} - \left(\zeta - \frac{a^2}{\bar{z}}\right)^{-1}\right\}. \tag{4}$$

This non-autonomous system of two coupled, nonlinear, ordinary differential equations defines the model system under study. The first term on the right-hand side of (4) gives the advecting velocity of the agitator at the position of the particle, the second term is the corresponding quantity due to the image. The apparent singularity when $z = 0$ can be removed by writing (4) as

$$\dot{\bar{\zeta}} = \frac{\Gamma}{2\pi i}\frac{|z|^2 - a^2}{(\zeta - z)(\zeta\bar{z} - a^2)}. \tag{4'}$$

A few elementary results about (4) and (4′) may be stated at once.

PROPOSITION 1: *The system* (4) *is Hamiltonian.*
This follows immediately by noting that, if

$$\zeta = \xi + i\eta, \tag{5}$$

where ξ, η are real, then (4) is equivalent to

$$\dot{\xi} = -\frac{\partial H}{\partial \eta}, \quad \dot{\eta} = \frac{\partial H}{\partial \xi}, \tag{6}$$

with

$$H = \frac{\Gamma}{2\pi}\log\left|\frac{\zeta - z}{\zeta - a^2/\bar{z}}\right|. \tag{7}$$

We are in essence just restating (3) here.

PROPOSITION 2: *The evolution governed by* (4) *induces a mapping of the disk* $|\zeta| \leqslant a$ *onto itself. This mapping is area-preserving.*
If T is some fixed time interval, the map is

$$\mathrm{M}: \zeta(t) \to \zeta(t + T)$$

and the results about M follow immediately from Proposition 1 and Liouville's theorem (cf. Khinchin 1949). In §3 this mapping will be constructed explicitly for a particularly simple stirring protocol $z(t)$.

PROPOSITION 3: *The system* (4) *is integrable if* (*a*) $z(t) = z_0$ *or* (*b*) $z(t) = z_0 \exp(i\Omega t)$.
In case (*a*), the Hamiltonian H, (7), is independent of time and we have an

autonomous system with one degree of freedom which is trivially integrable. In case (*b*) we set $\zeta = z\chi$. Then (4) reduces to

$$\dot{\bar{\chi}} - i\Omega\bar{\chi} = \frac{\Gamma}{2\pi i}\frac{1}{|z_0|^2}\left\{(\chi-1)^{-1} - \left(\chi - \frac{a^2}{|z_0|^2}\right)^{-1}\right\},$$

which is again integrable by an argument similar to that given for case (*a*). Note that this case contains case (*a*) (for $\Omega = 0$) and the case of a free vortex (when $\Omega = (\Gamma/2\pi)(|z_0|^2 - a^2)^{-1}$).

It is clear that the above results can be generalized to systems with more than one stirrer. If we have stirring vortices at $z_j(t), j = 1, \ldots, N$, with strengths $\Gamma_1, \ldots, \Gamma_N$, the generalization of (4) is simply

$$\dot{\bar{\zeta}} = \frac{1}{2\pi i}\sum_{j=1}^{N}\Gamma_j\left\{(\zeta - z_j)^{-1} - \left(\zeta - \frac{a^2}{\bar{z}_j}\right)^{-1}\right\}. \tag{8}$$

This system is again Hamiltonian. The generalization of (7) gives

$$H = \frac{1}{2\pi}\sum_{j=1}^{N}\Gamma_j \log\left|\frac{\zeta - z_j}{\zeta - a^2/\bar{z}_j}\right|. \tag{9}$$

The equations of motion for ζ are again integrable if $z_j(t) = z_j(0)\exp(i\Omega t)$ with the same Ω for all $j = 1, \ldots, N$. A key point here is that the number of stationary or uniformly rotating stirrers is irrelevant as far as integrability is concerned (compare §1). As we shall see in §4, it is the motion of a stirrer – and one is enough – that decides whether quasi-periodic or aperiodic (chaotic) particle trajectories are established.

To conclude this section, let us rewrite the model using dimensionless variables. We shall only consider stirrer motions of the form

$$z(t) = bf(t/T),$$

where $b < a$ is a constant amplitude and f is a real periodic function with period unity. That is, the stirrer oscillates back and forth between $+b$ and $-b$ according to our choice of the function f. If we now set

$$\zeta(t) = aZ(t/T)$$

we get

$$\dot{\zeta}(t) = \frac{a}{T}Z'\left(\frac{t}{T}\right),$$

where the prime denotes the derivative of Z with respect to its argument. Substituting these scaled expressions into (4′), we finally get

$$\frac{d\bar{Z}}{d\tau} = i\mu\frac{1-\beta^2 f^2}{(Z-\beta f)(\beta f Z - 1)},$$

where $\tau = t/T$ and

$$\beta = \frac{b}{a}, \tag{10}$$

$$\mu = \frac{\Gamma T}{2\pi a^2}. \tag{11}$$

The initial value $Z(0)$ should be chosen within the unit disk $|Z| \leqslant 1$. In the numerical work reported on in §4 we have chosen $a = 1$ and $\Gamma = 2\pi$ such that $\beta = b$ and $\mu = T$.

Our idealized model of stirring is thus completely parametrized by two dimensionless

quantities β and μ once the 'design', i.e. the form of the stirring function f, has been decided upon. The parameter β gives a dimensionless amplitude for the oscillations of the agitator. The parameter μ gives a dimensionless period of its motion. In §3 we shall discuss a particularly simple 'design'. Following that, in §4 we shall determine the efficiency of stirring (for that particular 'design') as a function of β and μ by numerical experiments.

3. The case of piecewise-constant stirrer motion

In this section we consider the particular case when

$$z(t) = \begin{cases} +b & (nT \leqslant t < (n+\frac{1}{2})T), \\ -b & ((n+\frac{1}{2})T \leqslant t < (n+1)T), \end{cases}$$

where $n = 0, \pm 1, \pm 2, \ldots$, and b and T are constants. This corresponds to a stirrer that jumps back and forth between fixed positions, or equivalently and more practically to a design in which two stirrers at fixed positions are run alternately for a given time interval.

During the time interval $0 \leqslant t < \frac{1}{2}T$ the particle motion is governed by the equation

$$\dot{\bar{\zeta}} = \frac{\Gamma}{2\pi i} \frac{b^2 - a^2}{(\zeta - b)(b\zeta - a^2)}, \tag{12}$$

and thus proceeds along an arc of a circle

$$\left| \frac{\zeta - b}{\zeta - a^2/b} \right| = \lambda, \tag{13}$$

where the value of the constant $\lambda, 0 < \lambda \leqslant b/a$, is given by ζ_0, the initial position of the marker. The radius of this circle is

$$\rho = \frac{\lambda}{1-\lambda^2}\left(\frac{a^2}{b} - b\right), \tag{14}$$

and its centre is at

$$\zeta_c = \frac{b - \lambda^2 a^2/b}{1-\lambda^2}. \tag{15}$$

For $\lambda = b/a$ the centre is at the origin and the radius $\rho = a$, i.e. the circle coincides with the boundary. For $\lambda \to 0$, $\rho \to 0$ and $\zeta_c \to b$.

We can now substitute

$$\zeta = \zeta_c + \rho e^{i\phi} \tag{16}$$

into (12) and obtain an equation of motion for ϕ. A straightforward calculation yields†

$$\dot{\phi}\left(1 - \frac{2\lambda}{1+\lambda^2}\cos\phi\right) = \frac{\Gamma}{2\pi\rho^2}\frac{1-\lambda^2}{1+\lambda^2},$$

which can immediately be integrated to give

$$\phi - \frac{2\lambda}{1+\lambda^2}\sin\phi = \frac{\Gamma}{2\pi\rho^2}\frac{1-\lambda^2}{1+\lambda^2}(t - t_0), \tag{17}$$

where $\phi = 0$ when $t = t_0$. The function

$$A_\lambda(\phi) = \phi - \frac{2\lambda}{1+\lambda^2}\sin\phi \tag{18}$$

† Note that $b - \zeta_c = \lambda\rho$ and $(a^2/b) - \zeta_c = \rho/\lambda$.

on the left-hand side of (17) is monotone since $\lambda < 1$ and its values are thus in a one-to-one correspondence with the angle ϕ through which the advected particle has been turned. In particular $A_\lambda(\phi) = \phi$ whenever $\phi = p\pi, p = 0, \pm 1, \pm 2, \ldots$. The period of rotation T_λ of the particle is given by

$$2\pi = \frac{\Gamma}{2\pi\rho^2}\frac{1-\lambda^2}{1+\lambda^2}T_\lambda \tag{19}$$

(the dependence of ρ on λ is given by (14)). Hence (17) is equivalent to the relation

$$\Delta A_\lambda(\phi) = 2\pi\Delta t/T_\lambda \tag{20}$$

which gives the change in $A_\lambda(\phi)$ during the time interval Δt.

A simple algorithm can now be stated which yields the position ζ_t of an advected particle at time $t \leqslant \frac{1}{2}T$ given its position ζ_0 at time $t = 0$. In accordance with (13) we first calculate λ from ζ_0 (and the values of a and b). We can then determine ζ_c from (15), and thus ρ and ϕ_0 from

$$\rho\, e^{i\phi_0} = \zeta_0 - \zeta_c$$

(cf. (16)). Next we use (20) in the form

$$A_\lambda(\phi_t) = A_\lambda(\phi_0) + 2\pi t/T_\lambda, \tag{21}$$

where $A_\lambda(\phi_0)$ is obtained from (18) and T_λ from (19). Equation (21) can be inverted – in practice by Newton's method – to give the polar angle, and finally then

$$\zeta_t = \zeta_c + \rho\, e^{i\phi_t}.$$

We shall use this algorithm for $t = \frac{1}{2}T$.

During the next half-cycle $\frac{1}{2}T \leqslant t < T$ the stirring vortex is at $z = -b$, and a similar calculation can be carried out to find ζ_T in terms of $\zeta_{\frac{1}{2}T}$. It is, however, more convenient to observe that ζ_T can be obtained by *first* inverting $\zeta_{\frac{1}{2}T}$ to obtain $-\zeta_{\frac{1}{2}T}$, *secondly* evolving $-\zeta_{\frac{1}{2}T}$ to $-\zeta_T$, using exactly the procedure just found when the stirrer is at $z = +b$, and *thirdly* constructing ζ_T from $-\zeta_T$ by another inversion. Figure 1 shows several sample trajectories, and in one case the points ζ_0, $\zeta_{\frac{1}{2}T}$ and ζ_T on a trajectory obtained by way of $-\zeta_{\frac{1}{2}T}$ and $-\zeta_T$ and the construction just described. We shall return to this construction and its significance in §5.1.

4. Numerical experiments

We now proceed to study the model of §3 by numerical computations in order to demonstrate the onset of chaotic motion and determine the relevant parameter values for this phenomenon to occur. The simplest way to do this is to iterate the mapping of Proposition 2 for a given set of initial marker positions and different parameter values. The time interval T in Proposition 2 will now be taken equal to the period of $z(t)$ in §3. As mentioned earlier (see the end of §2) we shall assume $\Gamma = 2\pi$, $a = 1$ so that $\beta = b$ and $\mu = T$.

Figure 2 shows some of the results. For all cases $\beta = 0.5$ and apparent qualitative differences result from varying the time interval $\mu\,(= T)$. The initial marker positions were in all cases as follows: nine markers uniformly spaced along the positive y-axis; six markers placed on the x-axis at $x = \pm 0.05, \pm 0.2, \pm 0.35$. For the smallest values of μ we see that the iterates fall on a family of level curves. The general shape of these curves can be understood by considering the advection due to two *fixed*, continuously operating vortex agitators, one at $z = +0.5$, the other at $z = -0.5$. The steady flow

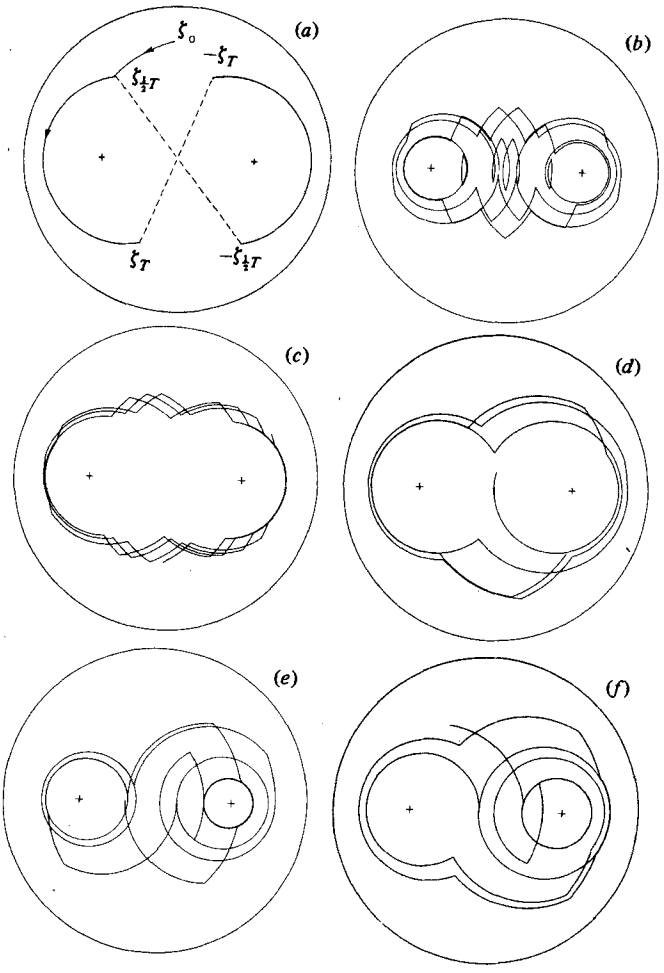

FIGURE 1. Sample particle trajectories for the model stirring device of §3. Parameters are $\beta = 0.5$ and $\mu = 1.5$ (*a–d*) or 0.5 (*e, f*). The construction discussed at the end of §3 and in §5.1 is illustrated in panel (*a*). Crosses indicate agitator positions.

generated in that case gives an integrable advected marker dynamics with pathlines and streamlines coinciding. This system of streamlines is shown in figure 3. It is clear that as $T \to 0$ (for fixed b, a and Γ) the model of §3 will look more and more like the two-fixed-agitator system; hence the similarities between figure 3 and figure 2(*a*). In fact, one may view the particle positions at times $2n(\frac{1}{2}T)$ and $(2n-1)(\frac{1}{2}T)$, where n is an integer, as the odd and even sets of coordinates in a 'leapfrog' scheme (with timestep $\frac{1}{2}T$) aimed at integrating the problem with two fixed stirrers numerically.† Thus one would expect 'convergence' as $T \to 0$. It is not implied by this that the chaos 'goes away' at some small but finite value of T. Rather, current ideas indicate that the size of the chaotic region goes to zero as $\exp(-\text{const}/T)$ for $T \to 0$. (The analogy also allows one to interpret the onset of chaos at larger values of T as a realization of the numerical instabilities to which the leapfrog scheme is susceptible at large stepsize. Similar interpretations appear in the recent work by Yamaguti & Oshiki (1981). However, for our present purposes this is a digression.)

† I am indebted to L. N. Howard for this remark.

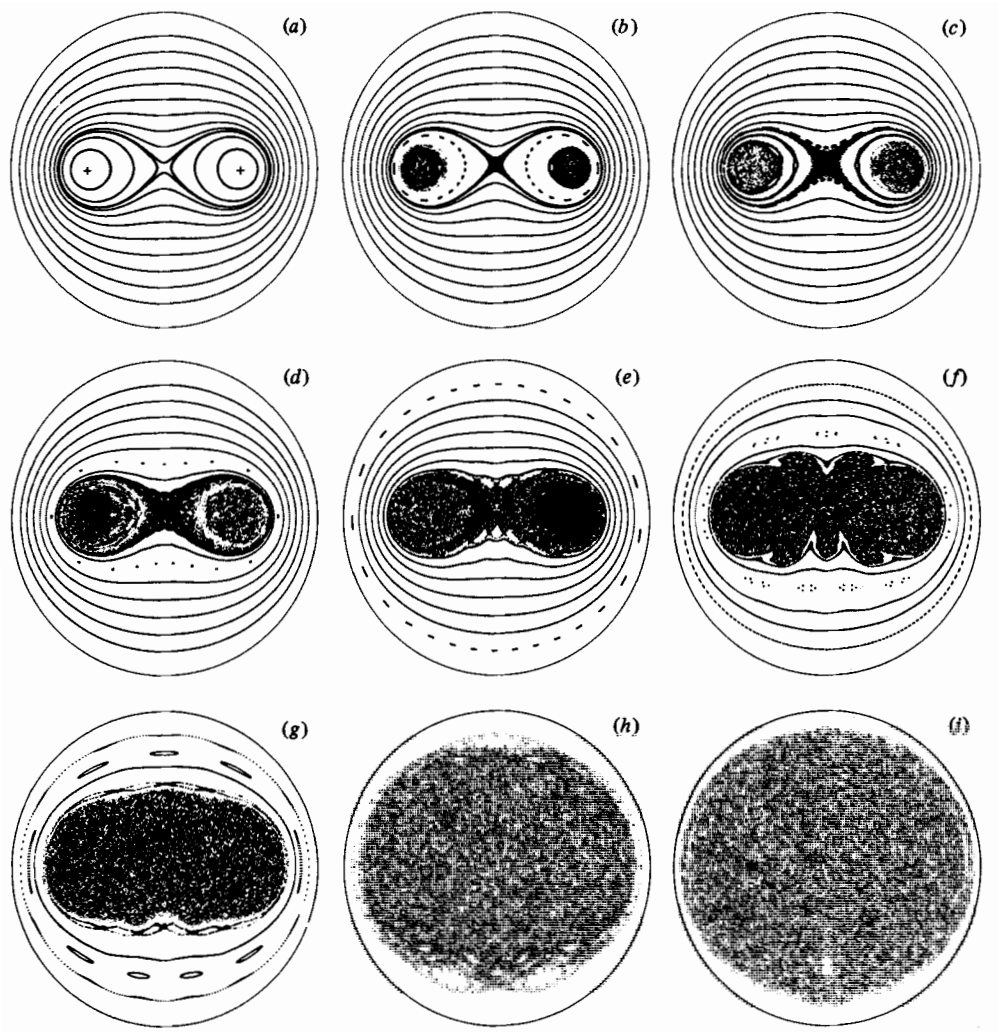

FIGURE 2. Iterated-map results described in §4. Parameters are $\beta = 0.5$ and (*a*) $\mu = 0.05$; (*b*) 0.10; (*c*) 0.125; (*d*) 0.15; (*e*) 0.20; (*f*) 0.35; (*g*) 0.50; (*h*) 1.0; (*i*) 1.5. Crosses indicate agitator positions.

As μ (or T) is increased, the innermost trajectories become erratic and the regular pattern of level curves is disrupted. As figure 2 shows, this disruption or instability to chaotic motion sets in when $\mu = 0.1$ and continues to consume a larger and larger portion of phase space, until at $\mu = 1.5$ no trace of regularity can be seen. It should be emphasized that for every value of μ we are simply iterating an explicitly given mapping for a predetermined number of steps. Hence increasing the value of μ does not increase the computational effort nor the reliability of the plotted points. (The accuracy to which the points are known is several orders of magnitude larger than the resolution of the plotter.) This is, of course, just a restatement of the standard advantages of a mapping over actual time integrations of differential equations. In a physical problem one commonly starts with a set of differential equations, such as (4), and it is sometimes difficult to specialize these equations so that an explicit analytical mapping emerges. One is then left with the option of constructing maps that *resemble* the system under study in some qualitative way, a procedure that has led to many important results, but which, clearly, from the point of view of any

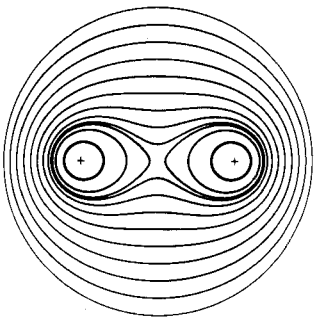

FIGURE 3. Streamlines for a device with two fixed agitators operating continuously. Agitators (indicated by crosses) are at $z = \pm 0.5a$, where a is the tank radius.

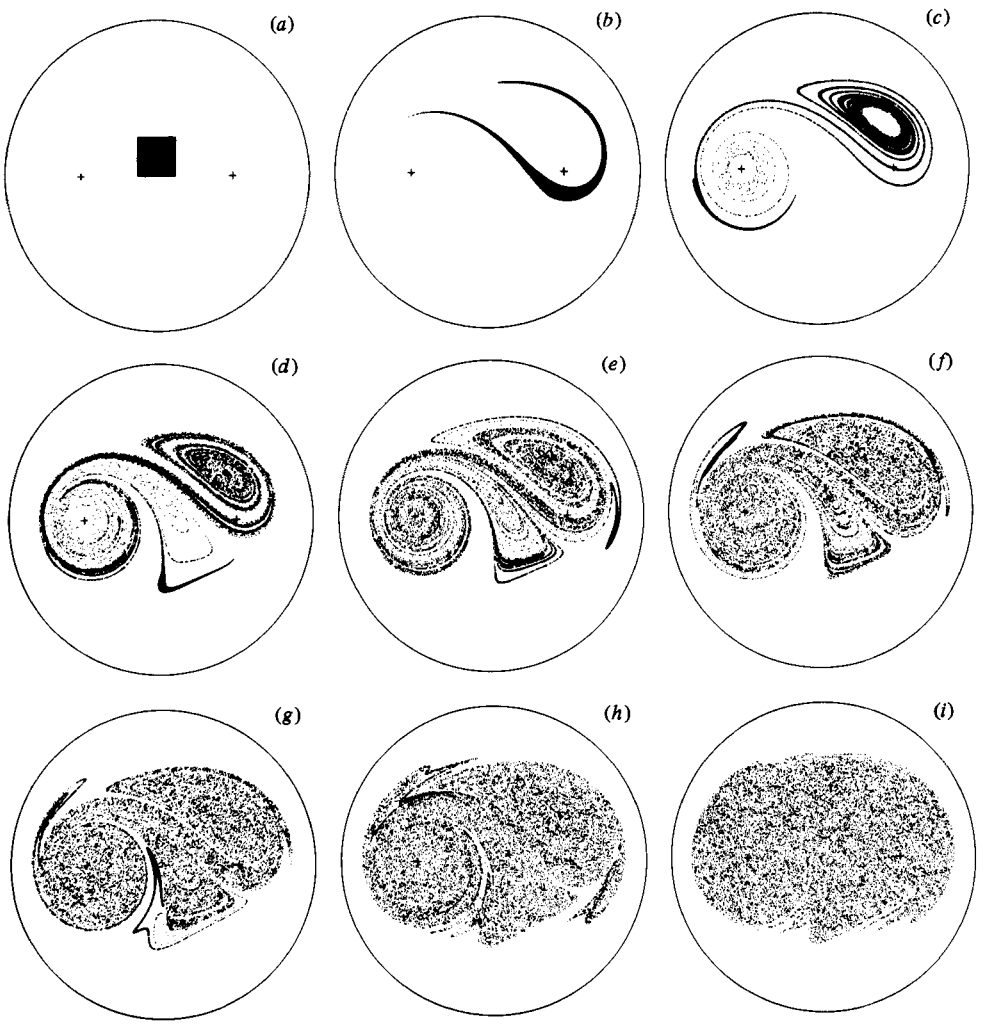

FIGURE 4. Phases in the stirring of an initially square array of particles. Parameters are $\beta = 0.5$, $\mu = 1.0$. Panels shown are at times (*a*) $t = 0$; (*b*) 1; (*c*) 2; (*d*) 3; (*e*) 4; (*f*) 5; (*g*) 6; (*h*) 9; (*i*) 12.

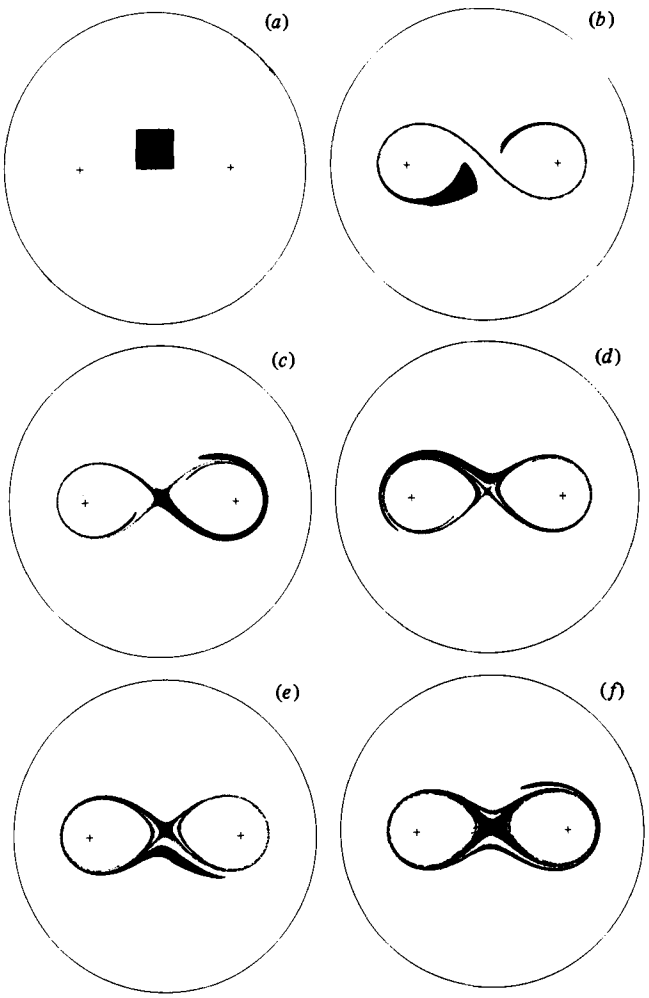

FIGURE 5. Phases in the stirring of an initially square array of particles. Parameters are $\beta = 0.5$, $\mu = 0.1$. Panels shown are at times (*a*) $t = 0$; (*b*) 1; (*c*) 2; (*d*) 3; (*e*) 4; (*f*) 12.

particular application leaves room for doubt about the relevance of the map results to the actual system. Here the reduction to a mapping is achieved by specializing the motion of the agitator to the non-differentiable alternating motion described in §3. For additional discussion of the relationship between differential equations ('flows') and maps see Lichtenberg & Lieberman (1983) and references therein.

It is important to realize what is being shown in figure 2 from the viewpoint of our intended application. If we calculate a fixed number of iterations, say 2000 (as is indeed done in figure 2), we are considering $2000 \times 0.05 = 100$ time units in figure 2(*a*) but 3000 time units in figure 2(*i*). In other words, in real time the 'stirring experiment' of figure 2(*a*) is essentially over before that in figure 2(*i*) has progressed substantially. What figure 2 shows us is that the nature of the stirring process for $T = 1.5$ is very different from that for $T = 0.05$. Indeed, if we take a blob of marked fluid and follow it as it is stirred, the parameters in figure 2(*a*) will lead to a predictable band (bounded by two streamlines in essence) within the tank wherein all this marked fluid may be found for all time. This is clearly not a very efficient way to operate

a stirring device. The parameters for figure 2(*i*), on the other hand, will lead to efficient stirring in the sense that marked particles may be found 'everywhere' in the tank after only a few stirring periods. As described below, numerical experiments show that on the order of 10 periods suffice. This result is in some ways counter-intuitive, since the more vigorous turning on and off of the two agitators (small T) might have been suspected of being the most efficient mechanism.

We now consider precisely this kind of stirring experiment which one would want to realize in a real device. We introduce a blob of fluid into the tank at time zero and watch it evolve. Figure 4 shows phases in the stirring of an initially square array of 10000 marker particles for the case $\beta = 0.5$, $\mu = 1.0$. The time elapsed between one frame and the next is one time unit ($T = \mu = 1.0$). We see that after about six time units the particles of the square have been distributed over a region† of the tank of size roughly comparable to the chaotic region seen in figure 2(*h*). From $t = 6$ to $t = 12$ the stirred blob is 'homogenized' over this region. Now compare this sequence of events to figure 5, which shows the same initial condition and geometry but with the agitation period set to $\mu = T = 0.1$, i.e. well inside the predominantly integrable regime (cf. figure 2*b*). The frames in figure 5 are at the same instants in real time as those of figure 4, i.e. we have waited for 10 stirring periods between one frame and the next. The configuration of advected particles at the final time in figure 5 is markedly different from that in figure 4. Although in figure 5 the particles have obviously been stirred about, they have not been able to wander throughout an extended region as in figure 4. They are, to use the terminology of the theory of dynamical systems, 'trapped between the tori of Kolmogorov, Arnold and Moser' (cf. Moser 1973; Berry 1978), and the model device does not stir effectively. The iterated maps in figure 2 clearly provide a useful diagnostic as to when the stirring device will be 'efficient' in the more traditional sense of figures 4 and 5. Similar runs were performed for $\mu = 2$ and $\mu = 3$. Again efficient stirring is seen with a larger stirred region as μ increases (see figure 6).

A number of runs of the type shown in figure 2 were performed for different values of the two dimensionless parameters β and μ (always keeping $\Gamma = 2\pi$ and $a = 1$), and, from the subjective impression created by the resulting images, each parameter pair was classified as leading to integrable (I), transitional (T) or chaotic (C) stirring. For example, for the sequence in figure 2 the value $\mu = 0.05$ was assigned the letter I, $\mu = 0.10$, 0.125 the letter T and all $\mu \geqslant 0.15$ the letter C. Collecting the assignments from all runs performed produced figure 7, which gives a crude indication of how the parameters should be chosen in order to achieve one of the three regimes listed. A couple of features of this figure are worthy of note. We have already remarked on the fact that integrability prevails as $T \to 0$ for fixed β. One might have suspected to find integrability as $T \to \infty$ for fixed β. This does not seem to be the case. If one is willing to wait long enough, efficient stirring will indeed take place. Keeping T (and hence μ) fixed we see that the system apparently is nonintegrable for sufficiently small β. This results from the fact that the model of §3 *without* the circular boundary shows a transition to chaotic behaviour as we shall discuss in §5.2. Finally as $\beta \to 1$ for fixed T the agitator and its image fuse, and one tends towards a state of no motion for all time.

We may construct a plot describing the onset of chaotic advection by measuring, again in a crude way, the size of the chaotic region for different values of the

† It is important to repeat that the mapping that led from figure 4(*a*) to figure 4(*i*) is *area-preserving*. For qualitative insights into the fate of a *curve*, e.g. the boundary of a certain fluid region, as it is stirred, see figure 10, which is discussed in §5.2. See also Aref & Tryggvason (1984).

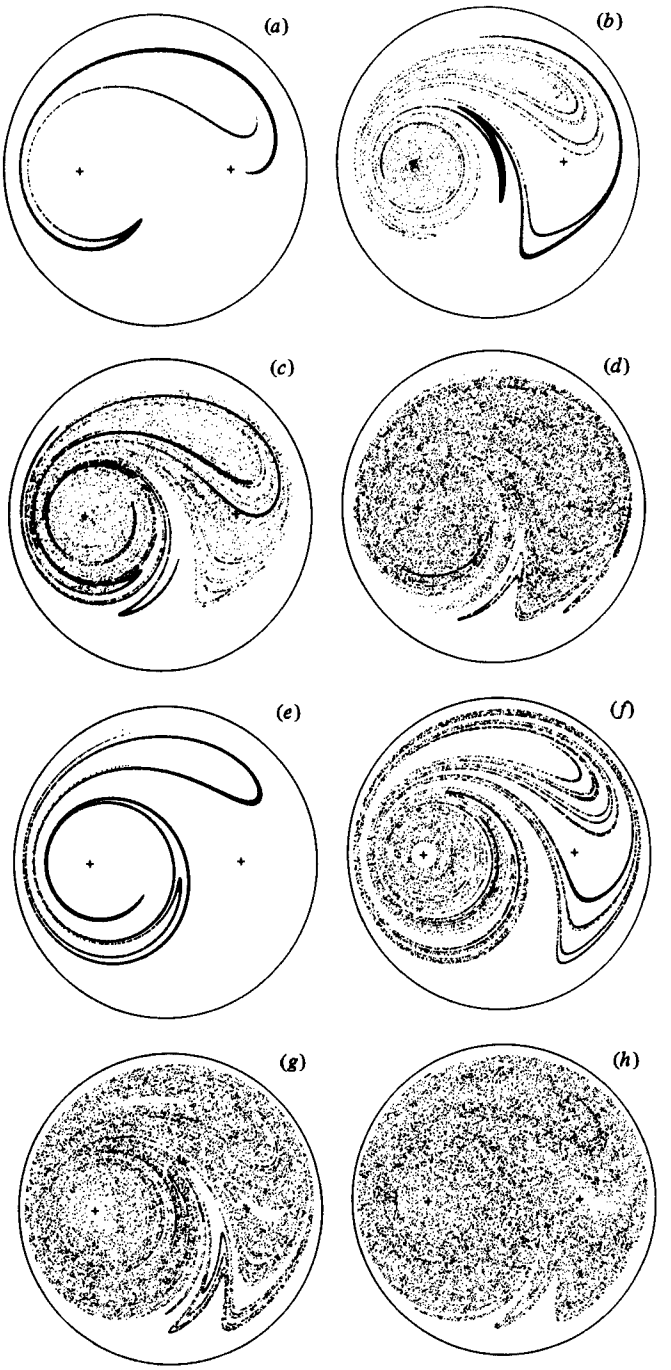

FIGURE 6. Phases in the stirring of an initially square array of particles. Same initial state as in figures 4 and 5. Parameters are $\beta = 0.5$ and $\mu = 2.0$ (*a–d*) or $\mu = 3.0$ (*e–h*). Panels shown are at times (*a*) $t = 2$; (*b*) 4; (*c*) 6; (*d*) 12; (*e*) 3; (*f*) 6; (*g*) 9; (*h*) 12.

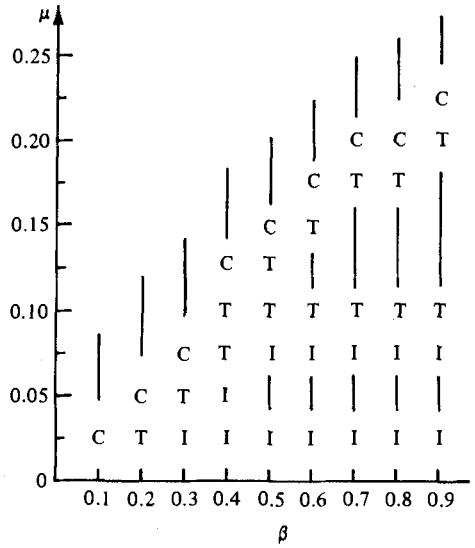

FIGURE 7. Classification of advection into 'integrable' (I), 'transitional' (T) or 'chaotic' (C) for the model stirring device as a function of the control parameters β and μ.

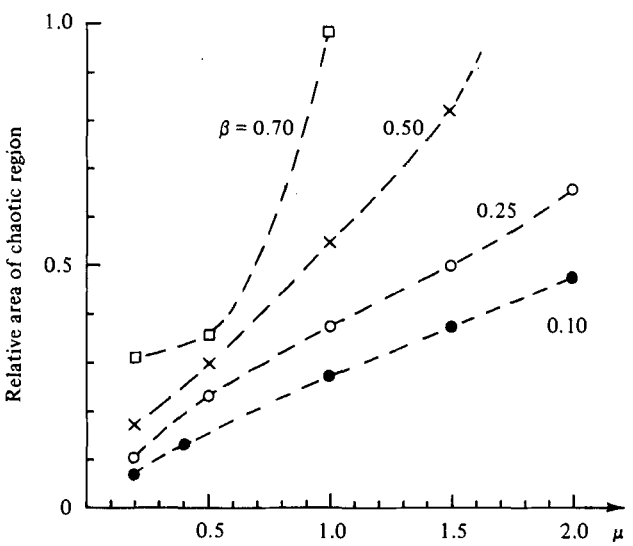

FIGURE 8. Growth of the size of the region displaying chaotic advection with μ for several values of β.

parameters. Figure 8 displays data of this type. The chaotic region was considered to be elliptical (cf. figure 2) and its minor and major axes were measured directly. In figure 8 we plot the product of these axes against the parameter μ for fixed β. A similar plot appears already in the investigation by Hénon & Heiles (1964). In our units the ordinate in figure 8 is the fraction of the area of the tank that is 'well stirred' for given parameters.†

We see that the rate at which the interior of the tank yields to chaotic orbits, i.e.

† This plot was suggested by J. B. Keller.

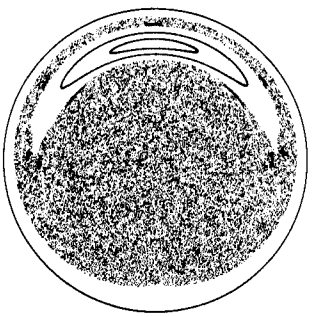

FIGURE 9. An 'island' of regular advection emerges within the chaotic region for $\beta = 0.1$, $\mu = 4.0$.

the slope of the curves in figure 8, depends on β. Clearly, from a practical point of view, one would wish to achieve a large region of chaotic advection at as low a value of T as possible (for fixed a and Γ). For the stirring protocol of §3 the slopes in figure 8 increase as β is increased. However, for $\beta \gtrsim 0.7$ the agitator is closer to its image than it is to the other agitator and the 'Poincaré section' changes character. The chaotic region becomes much more diffuse and its topology is now rather complicated. The crude measure used for figure 8 is no longer adequate. These remarks explain the restriction to $\beta \leqslant 0.7$ in figure 8.

It should also be mentioned that for small β and large μ regular 'islands' will sometimes re-emerge within the chaotic region. A very pronounced example is shown in figure 9, where $\beta = 0.1, \mu = 4.0$. A stable fixed point of the mapping has appeared, by symmetry on the y-axis, and a large neighbourhood of this fixed point consists of regular orbits. The small open patch on the y-axis in the lower portion of figure 2(*i*) is presumably the same phenomenon. The patch grows to about four times this size for $\mu = 2.0$ but has disappeared at $\mu = 2.5$. Regular 'islands' of this kind were ignored when generating figure 8.

5. Discussion

In this section we consider a number of issues relating to the formulation of the model and to the numerical results obtained.

5.1. *Connection with the theory of mappings*

As we have seen in the model of §3, a particle trajectory will consist of a sequence of circular arcs. Let $\mathrm{R}_+(\mu, \beta)$ denote the operator that performs the appropriate rotation about the stirrer position at $+b$. Thus the first part of a trajectory starting at ζ_0 results in a point

$$\zeta_1 = \mathrm{R}_+(\mu, \beta)\, \zeta_0, \tag{22}$$

where the notation signifies that R_+ depends on parameters μ, β and operates on ζ_0. Similarly we could introduce an operator $\mathrm{R}_-(\mu, \beta)$ to perform the rotation about the stirrer position $-b$. Then after a full period T the point ζ_0 would have moved to

$$\zeta_2 = \mathrm{R}_-(\mu, \beta)\, \zeta_1 = \mathrm{R}_-(\mu, \beta)\, \mathrm{R}_+(\mu, \beta)\, \zeta_0.$$

From now on we shall drop the arguments μ, β of $\mathrm{R}_\pm$. The construction mentioned at the end of §3 and illustrated in figure 1 amounts to the algebraic statement that

$$\zeta_2 = \mathrm{I}\mathrm{R}_+\mathrm{I}\mathrm{R}_+\, \zeta_0,$$

where I is the inversion in the origin: $I\zeta = -\zeta$. Thus for the full mapping $M = R_- R_+$ (cf. Proposition 2) we have the result

$$M = (IR_+)^2, \tag{23}$$

i.e. M is the *second iterate* of IR_+. This map IR_+, then, is really the basic entity in our problem.

As with all Hamiltonian maps IR_+ (and thus $M = (IR_+)^2$ itself) is *reversible* (Greene *et al.* 1981), which means that it can be written as a product of two involutions. It is not difficult to see explicitly how this comes about for the mapping IR_+. Consider the mappings S_x and S_y, which are the reflections in the x- and y-axes respectively:

$$S_x\zeta = \bar{\zeta}, \quad S_y\zeta = -\bar{\zeta}.$$

Now it is easy to see geometrically that

$$S_x R_+ = R_+^{-1} S_x. \tag{24}$$

Thus

$$IR_+ = (IR_+ S_y) S_y,$$

where, trivially, $S_y^2 = 1$ and

$$(IR_+S_y)^2 = IR_+S_yIR_+S_y = IR_+S_xR_+S_y = IR_+R_+^{-1}S_xS_y = I^2 = 1.$$

We have used (24) and the fact that $I = S_yS_x(= S_xS_y)$ in this derivation. It is possible to proceed with the theory of fixed points along the lines established in the literature (Greene *et al.* 1981), although the existence of a singularity (at $+b$) within the mapping domain creates some differences and difficulties. It is likely that scaling properties may be found for these model stirring devices following the recent work of Kadanoff (1981) and Shenker & Kadanoff (1982). Such developments may be somewhat more detailed than warranted by the present application.

5.2. *The case of no boundary*

If we simply ignore the bounding contour, we arrive at a very simple, explicitly given mapping.† Let the vortex positions still be $\pm b$. Then the speed of a particle starting at ζ_0 will be $\Gamma/2\pi|\zeta_0 - b|$, and in time $\frac{1}{2}T$ it will traverse a circular arc of angular spread $\Gamma T/4\pi|\zeta_0 - b|^2$ centred on the point $+b$. Hence, with the notation employed in §5.1,

$$\zeta_1 = b + (\zeta_0 - b)\exp\frac{i\Gamma T}{4\pi|\zeta_0 - b|^2}. \tag{25a}$$

Set

$$\zeta_1 = bZ_1, \quad \zeta_0 = bZ_0, \quad \tilde{\mu} = \frac{\Gamma T}{4\pi b^2};$$

then (25a) becomes

$$Z_1 = 1 + (Z_0 - 1)\exp\frac{i\tilde{\mu}}{|Z_0 - 1|^2}, \tag{25b}$$

which according to the results in §5.1 is to be followed by an inversion $Z_2 = -Z_1$. Thus in this simplified case we have reduced the problem to the study of a one-parameter map

$$\tilde{M}: Z \to Z', \tag{26a}$$

where

$$Z' = -1 + (1 - Z)\exp\frac{i\tilde{\mu}}{|1 - Z|^2}. \tag{26b}$$

† This first arose in a discussion with L. Merkine and J. T. C. Liu.

Numerical experiments with this explicit mapping show that it begins to display 'large-scale' chaotic behaviour when $\tilde{\mu} = \tilde{\mu}_c \approx 0.35$. Note that in terms of our earlier variables μ and β

$$\tilde{\mu} = \mu/2\beta^2.$$

Thus in the plot in figure 6 we must expect that the boundary between points marked T and points marked C converges to a parabola $\mu = 2\tilde{\mu}_c\beta^2$ as $\beta \to 0$. This is not inconsistent with what one actually finds, but the plot is too crude to check the relation sensitively.

The system considered here is presumably the simplest possible model in which chaotic advection (as defined in this paper) can be found. The explicit map (26) allows us to understand qualitatively the results of figure 2. For particles started very close to one of the agitators the dominant effect is the rotation by that agitator. The system with one agitator is, of course, integrable (even if the agitator is switched on and off), and the chaotic patches surrounding the agitators in figure 2 must come about from the perturbation of this one-agitator system by the distant second agitator. The situation is reminiscent of the perturbed twist-map theory of Moser (1973; see also Arnold & Avez 1968; Berry 1978), except that in the present system the rotation angle for the unperturbed case diverges as the singularity is approached. On the other hand, the evolution of chaos around the saddle point at the origin (cf. figures 2*a*, 3) and the general broadening of the separatrix ('figure of eight') streamline should undoubtedly be understood in terms of the theory of homoclinic points belonging to a hyperbolic fixed point (see Moser 1973; Berry 1978). Aspects of this process are computable using the Melnikov technique described by Holmes (1980) and by Holmes & Marsden (1982*a*, *b*).

In a noteworthy digression in their study of 'quantum maps', Berry *et al.* (1979) have actually already described, qualitatively, the different types of advection pattern presented here. They introduce the terminology of 'whorls' and 'tendrils', the former being associated with the vicinity of an elliptic fixed point, the latter with hyperbolic fixed points. To see these 'structures', consider the advection of a line of marker particles. Close to an elliptic fixed point, tightly wound spirals should appear owing to the difference in winding rate with distance from the fixed point. Examples of such spiral structures may be seen in the early stages of the sequences in figures 4 and 6. 'Tendrils' are the undulations that one should see as a line of marker is advected past a hyperbolic fixed point. They arise from the sinuous nature of the stable and unstable manifolds intersecting at an infinity of homoclinic points. Figure 10 provides four examples. A line down the middle of the tank (along the y-axis) consisting of 20000 particles was initialized and stirred. As it advects by the centre of the tank, the tendrils are clearly evident. The amplitude of the tendril oscillations increases with μ so that at $\mu = 0.5$ the tendrils in the centre of the tank and the 'whorls' about the agitators are inextricably bound together in a complex pattern. The evolution of tendrils on a closed contour and their influence on the degree of stretching of such a curve are elucidated in Aref & Tryggvason (1984).

We conclude by quoting from Berry *et al.* (1979): 'A typical [line of particles] may pass close to several elliptic and hyperbolic fixed points... and will therefore evolve into a fantastic shape incorporating both whorls and tendrils... Its curlings and flailings are reminiscent of cream spreading on coffee, and suggest that the study of generic area-preserving maps of curves on a plane, or surfaces in space, might be a profitable way to study turbulent mixing...'

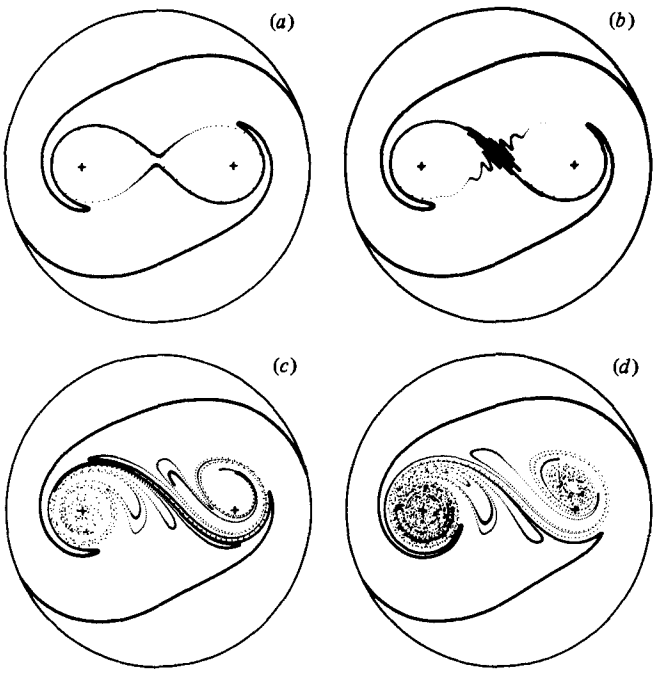

FIGURE 10. Evolution of 'tendrils' on an advected line of marker particles. For all cases $\beta = 0.5$, $t = 2$ and (a) $\mu = 0.1$; (b) 0.1; (c) 0.4; (d) 0.5. Note the 'whorls' in panel (c).

5.3. *Non-circular boundary*

We have already mentioned that the main virtue of a circular boundary is that it requires just one image for the stirring vortex. This property leads also to the result that, if the stirring vortex is a free vortex, thus precessing around inside the boundary at constant angular velocity, the advection problem is integrable. This situation, *viz* that the advection by a single free vortex in a bounded domain is an integrable problem, is probably restricted to the case of a circular boundary. We believe, as first conjectured by Novikov & Sedov (1979; see also Novikov 1980; Aref 1983), that for a 'general' boundary, advection by a single free vortex is chaotic. This conjecture has not so far been checked (much less proven). We suggest that advection in a rectangular 'container' with a free vortex would be an interesting problem. Putting fins and baffles on the inside of the circular boundary may also lead to relevant insights.

5.4. *Effects of viscosity, three-dimensionality etc.*

A number of objections (absence of viscosity, restriction to two-dimensionality etc.) can be raised to the simple model considered here when compared with realistic stirring devices. We shall completely exclude situations where a turbulent flow field is used as the agent of stirring and mixing since the type of flow we are considering is clearly to be classified as laminar. Indeed our flow is entirely deterministic (as emphasized in §1), whereas turbulent flows, used for advection or otherwise, are described stochastically.

We remark that it is possible to give examples of chaotic particle advection for a three-dimensional steady, incompressible, inviscid flow, i.e. the 'constraint' that the

advecting flow satisfies dynamical equations does not appear strong enough to rule out chaotic advection (in general) and in three dimensions steady flows suffice. Hénon (1966), following a suggestion by V. I. Arnold, studied the advection problem

$$\left.\begin{aligned} \dot{x} &= A\sin z + C\cos y, \\ \dot{y} &= B\sin x + A\cos z, \\ \dot{z} &= C\sin y + B\cos x \end{aligned}\right\} \tag{27}$$

for $A = \sqrt{3}, B = \sqrt{2}, C = 1$. For any values of the constants A, B, C the incompressible flow on the right-hand side of (27) is a steady solution of the three-dimensional Euler equation. Hénon's (1966) numerical results indicate regions of chaotic behaviour for the advection which should translate into efficient stirring and mixing. For a recent, highly mathematical study of related advection problems see Broer (1981).

The effects of viscosity present us with somewhat more complicated problems. Basically a new physical entity, the kinematic viscosity ν, would be introduced. We then have a new dimensionless quantity Γ/ν, which turns out just to be the Reynolds number written in a somewhat unconventional form. Our analysis in the preceding sections might then be expected to apply in the limit $\nu \ll \Gamma$. However, we recall that the steady viscous flow about a uniformly rotating cylinder in unbounded fluid has precisely the same form as the flow produced by a line vortex coincident with the axis of the cylinder. Furthermore, the rapidity with which the steady state is achieved increases as the fluid becomes more viscous, as does the rate at which a circulatory motion is damped once the cylinder stops rotating. These remarks suggest an approximate realization of the model device of §3 using two cylinders, that are set into rotation alternately, and a rather viscous fluid. This reminds one of the device used by Taylor (1972) in his film to demonstrate reversibility of low-Reynolds-number flow. The two-cylinder device would, of course, be reversible in principle (just as the mapping in the model is reversible) but, because of the nonintegrability of particle motion and the consequent sensitivity to slight variations in particle position, it would probably be impossible to unscramble a stirred blob of coloured fluid after even a few periods by turning the cylinders backwards. This behaviour could then be contrasted with Taylor's (1972) demonstration.†

5.5. '*Entrainment diagrams*'

The idea that concepts of dynamical-systems theory, such as critical points and their bifurcations, are useful to the analysis of real-space flow patterns has been promoted by Perry & Fairlie (1974) and more recently by Cantwell (1981*a*, *b*). The idea is not unnatural, since, in fact, the names used in the theory of dynamical systems for various singularities of phase-plane flows were originally derived from hydrodynamic terminology (*viz* source, sink, vortex, the interpretation of Liouville's theorem as a statement of incompressibility of phase-space flow, etc.). The work just mentioned is aimed at Lagrangian characteristics of the advected particle motion (as is this paper). However, it is concerned with situations in which the advection problem can be reduced to an *autonomous* system consisting of two coupled ordinary differential equations. This is achieved by invoking flows with particular symmetries, e.g. axisymmetry, and also by making use of similarity properties of the solution. Thus, in particular, the flows analysed by Cantwell (1981*a*, *b*; see also Cantwell, Coles & Dimotakis 1978, in particular the Appendix) need not be steady (in the usual sense)

† This paragraph was influenced by remarks of T. Maxworthy after the presentation in Aref (1982*b*). A two-cylinder device actually appears in figure 163 of the early treatise by Bouasse (1931).

but by adopting certain similarity variables the equations of motion for a particle are reduced to the aforementioned form. Critical points of the flow pattern are now identified, and their bifurcations as the Reynolds number is varied are studied. Cantwell (1981*a*) has introduced the term *entrainment diagrams* for the 'phase portraits' that ensue.

The present investigation is in many ways closely allied to this work. However, a principal result in this paper is that two-dimensional 'steady' (in a broad sense, i.e. including the possibility of similarity variables) advection and two-dimensional unsteady advection are radically different processes. The former is integrable, the latter, in general, is not. In this sense the results presented here are complementary to those of Perry & Fairlie (1974) and Cantwell (1981*a*,*b*), and show that the entrainment diagrams should be considered very special cases of particle advection, just as laminar solutions of the Navier–Stokes equations form but a small and specialized subset of all solutions, the preponderance of which correspond to turbulent flow. An important point is that for the advection problem chaotic solutions need not correspond to turbulent flows. Very regular flows (in the sense that the Eulerian field has a simple time dependence) can lead to highly irregular advection patterns. One has no notion of this from the entrainment diagrams.

This remarkable contrast between the Eulerian and Lagrangian representation of the same flow was apparent to Amsden & Harlow (1964), while performing numerical simulations using the particle-in-cell method where particles are advected in a prescribed flow known at the sites of a grid. They refer very aptly to 'the relative orderliness of Eulerian representation over Lagrangian'. Interpretations of flow-visualization pictures face this problem routinely. Given the marker dispersion in figure 4(*i*) the problem is to determine the source(s) of agitation. In general, owing to chaotic advection, this inverse problem is impossible to solve!

I am indebted to N. Pomphrey for discussions on the restricted four-vortex problem that is so intimately connected with this work. I also wish to thank E. P. Flinchem, D. Q. Larkin and G. Tryggvason for constructive comments.

This research was supported by National Science Foundation grant MEA 81-16910 to Brown University. The provision of computer resources by the Scientific Computing Division at the National Center for Atmospheric Research is gratefully acknowledged. NCAR is sponsored by NSF.

REFERENCES

Amsden, A. A. & Harlow, F. H. 1964 Slip instability. *Phys. Fluids* **7**, 327–334.

Aref, H. 1982*a* An idealized model of stirring. *Woods Hole Oceanogr. Inst. Tech. Rep.* WHOI-82-45, pp. 188–189.

Aref, H. 1982*b* Stirring by chaotic advection. *Bull. Am. Phys. Soc.* **27**, 1178 (abstract only).

Aref, H. 1983 Integrable, chaotic, and turbulent vortex motion in two-dimensional flows. *Ann. Rev. Fluid Mech.* **15**, 345–389.

Aref, H. & Pomphrey, N. 1980 Integrable and chaotic motions of four vortices. *Phys. Lett.* **A78**, 297–300.

Aref, H. & Tryggvason, G. 1984 Vortex dynamics of passive and active interfaces. *Physica* **D** (to appear).

Arnold, V. I. & Avez, A. 1968 *Ergodic Problems of Classical Mechanics.* Benjamin.

Batchelor, G. K. 1967 *An Introduction to Fluid Dynamics.* Cambridge University Press.

Berry, M. V. 1978 Regular and irregular motion. *AIP Conf. Proc.* no. 46, 16–120.

Berry, M. V., Balazs, N. L., Tabor, M. & Voros, A. 1979 Quantum maps. *Ann. Phys.* **122**, 26–63.

BOUASSE, H. 1931 *Tourbillons*, Vol. 1. Librairie Delagrave, Paris.

BROER, H. 1981 Quasi-periodic flow near a codimension one singularity of a divergence free vector field in dimension three. In *Dynamical Systems and Turbulence, Warwick 1980* (ed. D. A. Rand & L.-S. Young). Lecture Notes in Mathematics, vol. 898, pp. 75–89. Springer.

CANTWELL, B. J. 1981*a* Organized motion in turbulent flow. *Ann. Rev. Fluid Mech.* **13**, 497–515.

CANTWELL, B. J. 1981*b* Transition in the axisymmetric jet. *J. Fluid Mech.* **104**, 369–386.

CANTWELL, B. J., COLES, D. & DIMOTAKIS, P. 1978 Structure and entrainment in the plane of symmetry of a turbulent spot. *J. Fluid Mech.* **87**, 641–672.

CHANDRASEKHAR, S. 1943 Stochastic problems in physics and astronomy. *Rev. Mod. Phys.* **15**, 1–89.

FRIEDRICHS, K. O. 1966 *Special Topics in Fluid Dynamics*. Gordon & Breach.

GREENE, J. M., MACKAY, R. S., VIVALDI, F. & FEIGENBAUM, M. 1981 Universal behavior in families of area-preserving maps. *Physica* **D3**, 468–486.

HÉNON, M. 1966 Sur la topologie des lignes de courant dans un cas particulier. *C. R. Acad. Sci. Paris* A **262**, 312–314.

HÉNON, M. & HEILES, C. 1964 The applicability of the third integral of motion: some numerical experiments. *Astron. J.* **69**, 73–79.

HOLMES, P. J. 1980 Averaging and chaotic motions in forced oscillations. *SIAM J. Appl. Maths* **38**, 65–80.

HOLMES, P. J. & MARSDEN, J. E. 1982*a* Horseshoes in perturbations of Hamiltonian systems with two degrees of freedom. *Commun. Math. Phys.* **82**, 523–544.

HOLMES, P. J. & MARSDEN, J. E. 1982*b* Melnikov's method and Arnold diffusion for perturbations of integrable Hamiltonian systems. *J. Math. Phys.* **23**, 669–675.

KADANOFF, L. P. 1981 Scaling for a critical Kolmogorov–Arnold–Moser trajectory. *Phys. Rev. Lett.* **47**, 1641–1643.

KHINCHIN, A. I. 1949 *Mathematical Foundations of Statistical Mechanics*. Dover.

LAMB, H. 1932 *Hydrodynamics*, 6th edn. Dover.

LICHTENBERG, A. J. & LIEBERMAN, M. A. 1983 *Regular and Stochastic Motion*. Springer.

MOSER, J. 1973 *Stable and Random Motions in Dynamical Systems*. Princeton University Press.

NOVIKOV, E. A. 1980 Stochastization and collapse of vortex systems. *Ann. N.Y. Acad. Sci.* **357**, 47–54.

NOVIKOV, E. A. & SEDOV, YU. B. 1979 Stochastization of vortices. *JETP Lett.* **29**, 677–679.

PERRY, A. E. & FAIRLIE, B. D. 1974 Critical points in flow patterns. *Adv. Geophys.* **18**, 299–315.

PRANDTL, L. & TIETJENS, O. G. 1934 *Fundamentals of Hydro- and Aeromechanics*. Dover.

RICHARDSON, L. F. 1926 Atmospheric diffusion on a distance neighbour graph. *Proc. R. Soc. Lond.* A **110**, 709–737.

SHENKER, S. J. & KADANOFF, L. P. 1982 Critical behavior of a KAM surface: I. Empirical results. *J. Stat. Phys.* **27**, 631–656.

TAYLOR, G. I. 1921 Diffusion by continuous movements. *Proc. Lond. Math. Soc.* **20**, 196–211.

TAYLOR, G. I. 1972 Low-Reynolds-number flows. In *Illustrated Experiments in Fluid Mechanics*, pp. 47–54. MIT Press. Also 16 mm sound film distributed by Encyclopedia Britannica Educational Corporation.

WHITTAKER, E. T. 1937 *A Treatise on the Analytical Dynamics of Particles and Rigid Bodies*, 4th edn. Cambridge University Press.

YAMAGUTI, M. & OSHIKI, S. 1981 Chaos in numerical analysis of ordinary differential equations. *Physica* **D3**, 618–626.

ZIGLIN, S. L. 1980 Nonintegrability of a problem on the motion of four point vortices. *Sov. Math. Dokl.* **21**, 296–299.